

Theory of commensurable magnetic structures in holmium

Jens Jensen

Ørsted Laboratory, Niels Bohr Institute, Universitetsparken 5, 2100 Copenhagen, Denmark

(September 12, 2018)

Abstract

The tendency for the period of the helically ordered moments in holmium to lock into values which are commensurable with the lattice is studied theoretically as a function of temperature and magnetic field. The commensurable effects are derived in the mean-field approximation from numerical calculations of the free energy of various commensurable structures, and the results are compared with the extensive experimental evidence collected during the last ten years on the magnetic structures in holmium. In general the stability of the different commensurable structures is found to be in accord with the experiments, except for the $\tau = 5/18$ structure observed a few degrees below T_N in a *b*-axis field. The trigonal coupling recently detected in holmium is found to be the interaction required to explain the increased stability of the $\tau = 1/5$ structure around 42 K, and of the $\tau = 1/4$ structure around 96 K, when a field is applied along the *c*-axis.

75.10.-b 75.25.+z 75.30.Gw

I. INTRODUCTION

The basic features of the magnetically ordered structures in hexagonal close-packed Ho were established by Koehler *et al.*,¹ who found that the basal-plane moments are arranged in a helical pattern at all temperatures below $T_N \simeq 133$ K. The *c*-axis components order ferromagnetically at $T_C \simeq 20$ K, resulting in a conical ordering of the moments. The opening angle of the cone was found to approach 80° in the zero temperature limit. The ordering wave vector for the basal-plane moments is directed along the *c*-axis and its magnitude τ (in units of $2\pi/c$) was observed to change monotonically from about 0.28 at T_N to about $0.167 \simeq 1/6$ at T_C . Below T_C the wave vector stays constant, indicating that the magnetic structure is locked to the lattice periodicity and repeats itself after each twelve hexagonal layers. The hexagonal anisotropy is known² to produce higher harmonics at $(6 \pm 1)\tau$, and the fifth and seventh harmonics were clearly resolved by Koehler *et al.* at low temperatures. They concluded that the basal-plane moments in the cone phase bunch strongly around the easy *b*-directions, so that the angle between the basal-plane component of one of the moments and the nearest *b*-axis is only about 5.8° in the zero temperature limit. The neutron diffraction experiments have been repeated with higher resolution and with crystals of better quality by Felcher *et al.*³ and by Pechan and Stassis,⁴ leading to only minor modifications of the results of Koehler *et al.*

Koehler and collaborators⁵ also investigated the behavior of the magnetic structure in holmium as a function of magnetic field applied in the basal plane. The theoretical prediction for the magnetization process was that the helix would change into a ferromagnet either directly or via an intermediate fan phase.⁶ This was confirmed to occur at low temperatures, however, above 40–50 K Koehler *et al.* observed a second fan-like phase.⁵ A few years ago this extra intermediate phase was explained, as being the helifan(3/2)-phase,^{7,8} where the helifan structures are constructed from portions of the helix and the fan following each other in a periodic way.

The next major advancement in the investigation of the magnetic ordering in holmium

came with the use of the new technique of magnetic x-ray scattering, which utilizes the intense radiation from a synchrotron source. The narrow experimental resolution obtainable with this technique made it possible for Gibbs *et al.*⁹ to detect two other commensurable structures in holmium, with $\tau = 2/11$ and $5/27$, in addition to the one with $\tau = 1/6$, at temperatures below 25 K. These commensurable values were explained by the spin-slip model.^{9,10} In the limit of very strong hexagonal anisotropy the moments would be confined to be aligned along one of the six (in the present case) *b*-directions. The 12-layered structure may be constructed from pairs of neighboring layers, in which the moments are along the same *b*-direction, by allowing the moments to rotate 60° from one pair to the next. This periodicity may then be changed by introducing regularly-spaced series of *spin slips*, where at each spin slip a pair is replaced by a single layer. For example, the 22 layered 2/11-structure may be obtained from the 12-layered structure by introducing a spin slip after every 5 pair of layers, which we shall denote as the (222221)-structure. The introduction of a spin slip after every 4 pairs leads to the (22221)-structure corresponding to $\tau = 5/27$. In this structure there is a spin slip for every 9 layers, and as observed by Gibbs *et al.*, this gives rise to a modulation of the lattice with this period, i.e. charge scattering at $\tau_c = 2/9$.

The magnetic x-ray scattering technique provides very good resolution, but the intensity is weak, thus preventing the measurement of the scattering due to the higher harmonics. In contrast, neutron diffraction reflections have high intensities, although the resolution is relatively coarse. By the use of a large Ho-crystal, and a triple-axis neutron-scattering spectrometer for isolating the purely elastic scattered neutrons, Cowley and Bates were able to determine the intensities due to all the harmonics in a number of the spin-slip structures, in which the intensities extend over four orders of magnitude.¹¹ These results allowed them to derive the average turn angle between the bunched pairs to be about 10° at the low temperatures, in accordance with the result of Koehler *et al.*,¹ and this value increases to about 20° at 30 K. In addition they were able to detect some variation of the turn angle from pair to pair. The magnitudes of the two modifications of the ideal spin-slip structure which were derived from the experiments were reproduced in a numerical model calculation.¹²

The ultrasonic experiments made by Bates, *et al.*¹³ as a continuation of the experiments of Cowley and Bates, showed anomalies in the sound velocities not only at the temperatures where the system jumps between the three commensurable structures described above, but also at about 25, 40 and 97 K. At these latter temperatures τ is close to the commensurable values $4/21$, $1/5$, and $1/4$, corresponding to the spin slip structures (2221), (221), and (211), respectively.

The possibility that the magnetic structure may lock into commensurable values at elevated temperatures was investigated at Chalk River by Tindall, Steinitz and collaborators.^{14–24} They monitored the position of the fundamental magnetic diffraction peak as a function of temperature at fields applied along the *c*-direction or along the *b*-direction, and they found several plateaus in the temperature variation of τ . In the presence of a *c*-axis field of 30 kOe the (221)- and the (211)-structures were found to be stable around 42 K and 96 K, respectively, in both cases within a temperature interval of 2–3 K. In a *b*-axis field of 14 or 30 kOe the (211)-structure is again stable for a couple of degrees, which was also observed to be the case for the (21)-structure, $\tau = 2/9$, at about 75 K. Finally, they observed τ to stay close to the value $5/18$ between 126 K and the Néel temperature, when applying a field of 30 kOe along the *b*-axis. The observations made close to T_N and near 100 K have largely been confirmed by the similar experiments of Venter and du Plessis,^{25,26} except that they did not observe a clear plateau at $\tau = 1/4$ in a *c*-axis field around 96 K. However, they detected an anomalous behavior of the scattering intensity close to this temperature.

The low temperature domain, below 40 K, has been carefully investigated by Cowley *et al.*²⁷ in a *c*-axis field of 10–50 kOe. In spite of a rather monotonic variation, with field or temperature, of the position of the fundamental magnetic satellite they found by measuring the position of the higher harmonics that the diffraction pattern was determined in many cases by a superposition of neutrons scattered from domains with different commensurable τ -values. Small differences in τ , which may be difficult to resolve at the fundamental wave vectors, are enhanced so to be distinguishable when considering e.g. the fifth or seventh

harmonics.

There have been made a number of theoretical studies of commensurable structures in model systems. The simplest one, the anisotropic next-nearest-neighboring Ising (ANNI) model has been investigated in detail both at zero field^{28–30} and in an applied field.³¹ The XY-model with six-fold anisotropy, which is more closely related to holmium, has recently been discussed by Sasaki,³² in the limit of large anisotropy, and by Seno *et al.*³³ Steinitz *et al.*³⁴ have made some qualitative considerations on the connection between the spin-slip model and the field-dependent commensurable effects observed in holmium. Plumer has analyzed a model, which includes most of the couplings present in holmium, in order to understand the stability of the 1/4-phase observed near 96 K in a *c*-axis field.³⁵ However, the explanation he proposed, relies on adding a large symmetry-breaking term to the free energy which seems difficult to justify. Here we shall present a mean-field calculation of the stability of the different commensurable phases based on a realistic model for holmium. The model includes not only the terms considered by Plumer, but also the trigonal coupling which has recently been detected in neutron diffraction measurements by Simpson *et al.*³⁶ The trigonal coupling induces a net ferromagnetic moment in the basal plane when $\tau = 1/4$, and a misalignment of the field by as little as one degree is sufficient for explaining the observed lock-in of this structure, in accordance with the conjecture made by Jensen and Mackintosh.³⁷ The basal-plane three-fold anisotropy caused by the trigonal coupling in the case of a cone structure has also strong implications on the (221)-structure in a *c*-axis field near 42 K.

The model used in the calculations is developed in the next section. The stability of the different commensurable structures is investigated in Sec. III. The free energy of the various structures is calculated numerically within the mean-field approximation. The advantage of this method is that it is possible to account for most of the complexities of the real system, whereas one disadvantage is that there is a limit to the number of different layers one may handle numerically with the sufficient precision. In the present calculations we consider structures with a repeat length of up to 500 layers, leading to a resolution which should be

superior to even the most precise experiments. The work is summarized and concluded in the last Sec. IV.

II. THE MEAN-FIELD MODEL OF HOLMIUM

The model is based on the magnetization and spin-wave measurements, and is similar to the one applied in previous numerical analyses of the magnetic structures and excitations in holmium.^{7,12,37–41} The Hamiltonian comprises the single-ion anisotropy, the Zeeman term, the Heisenberg exchange coupling, the classical magnetic dipole–dipole interaction, and the trigonal coupling:

$$\begin{aligned} \mathcal{H}_0 = & \sum_i \sum_{lm} B_l^m O_l^m(i) - \sum_i g\mu_B \mathbf{H} \cdot \mathbf{J}_i \\ & - \frac{1}{2} \sum_{ij} \mathcal{J}(ij) \mathbf{J}_i \cdot \mathbf{J}_j - \frac{1}{2} \sum_{ij} \mathcal{J}_D(ij) J_{zi} J_{zj} \\ & + \sum_{ij} K_{21}^{31}(ij) [O_3^2(i) J_{yj} + O_3^{-2}(i) J_{xj}]. \end{aligned} \quad (2.1)$$

The O_l^m -operators are the Stevens operators, and in particular $O_3^{\pm 2} = \frac{1}{2}(J_z O_2^{\pm 2} + O_2^{\pm 2} J_z)$, where $O_2^2 = J_x^2 - J_y^2$ and $O_2^{-2} = J_x J_y + J_y J_x$. The x -, y -, and z -axes are assumed to be along the a -, b -, and c -axes of the HCP lattice, respectively. The Fourier transforms of the couplings are defined in the standard way, and we shall use the short hand notation $\mathcal{J}(q)$ for $\mathcal{J}(\mathbf{q})$, when \mathbf{q} is along the c -axis. The inter-planar exchange parameters \mathcal{J}_n are then defined by

$$\mathcal{J}(q) = \mathcal{J}_0 + 2 \sum_{n \geq 1} \mathcal{J}_n \cos(nqc/2). \quad (2.2)$$

The classical dipole interaction is included in the coupling $\mathcal{J}(q)$ of the basal-plane moments, in which case the coupling of the c -components is $\mathcal{J}_{cc}(q) = \mathcal{J}(q) + \mathcal{J}_D(q)$. The classical contribution vanishes at zero wave vector, $\mathcal{J}_D(\mathbf{0}) \equiv 0$, whereas at $q \neq 0$

$$\begin{aligned} \mathcal{J}_D(q) = & \\ & - \mathcal{J}_{dd} \{0.919 + 0.0816 \cos(qc/2) - 0.0006 \cos(qc)\}, \end{aligned} \quad (2.3)$$

where the coupling constant in holmium is

$$\mathcal{J}_{dd} = 4\pi(g\mu_B)^2 N/V = 0.0349 \text{ meV}. \quad (2.4)$$

The jump, which the dipole coupling $\mathcal{J}_D(q)$ makes at zero wave vector, is observable in the excitation spectrum, and it explains without introducing any further two-ion anisotropy,³⁸ why the system prefers the cone structure rather than the “tilted helix” below T_C .

The trigonal coupling was discovered to be present in erbium by Cowley and Jensen.⁴² This coupling reflects the fact that the c -axis is a three-fold symmetry axis, and its contribution to the mean-field Hamiltonian for the i th ion is given by

$$\begin{aligned} \Delta\mathcal{H}_{MF}(i \in p\text{'th plane}) = & (-1)^p \sum_{n \geq 1} [K_{31}^{21}]_n \\ & \times \left[\{O_3^2(i) - \frac{1}{2}\langle O_3^2(i) \rangle\} \langle J_y(p+n) - J_y(p-n) \rangle \right. \\ & + \{O_3^{-2}(i) - \frac{1}{2}\langle O_3^{-2}(i) \rangle\} \langle J_x(p+n) - J_x(p-n) \rangle \\ & - (-1)^n \{J_{yi} - \frac{1}{2}\langle J_{yi} \rangle\} \langle O_3^2(p+n) - O_3^2(p-n) \rangle \\ & \left. - (-1)^n \{J_{xi} - \frac{1}{2}\langle J_{xi} \rangle\} \langle O_3^{-2}(p+n) - O_3^{-2}(p-n) \rangle \right], \end{aligned} \quad (2.5)$$

where the argument $p \pm n$ denotes an ion in the uniformly magnetized $(p \pm n)$ th hexagonal layer. This equation, which defines the inter-planar coupling parameters $[K_{31}^{21}]_n$, shows that the coupling changes sign from one sublattice to the next. Both in the cone phase and in the cycloidal phase of erbium, the trigonal coupling gives rise to additional neutron diffraction peaks when the scattering vector is along the c -axis. These peaks would not be there if the magnetic structures were independent of the different orientation of the basal planes in the two hexagonal sublattices. The equivalent phenomenon has also now been observed in holmium by Simpson *et al.*,³⁶ who fitted the intensities of the extra reflections by a set of three inter-planar parameters for the trigonal coupling.

We have reanalyzed the experiments of Simpson *et al.*³⁶ and derived a set of anisotropy parameters, which accounts both for the low temperature magnetization curves, as precisely as the previous model,³⁸ and for the neutron diffraction results. The effects of all

the three trigonal couplings of the fourth rank,⁴² and combinations of the three couplings were investigated, and in agreement with Simpson *et al.* we find that the trigonal coupling introduced by Eq. (2.5) (the coupling applied in erbium), is the one which leads to the best fit. The small differences between the ways the neutron diffraction results are fitted are insignificant compared with the experimental uncertainties, but the inter-planar coupling parameters derived here are, quite remarkably, a factor of 4-5 smaller than those obtained by Simpson *et al.* This large difference is surprising, but may be explained by the high degree of compensation which occurs between the different terms in the mean-field Hamiltonian (2.5). The degree of compensation depends on the structure considered, and in the analysis of the commensurable structures discussed in the next section we found that the trigonal coupling derived by Simpson *et al.* has unacceptably strong implications in some cases. The alternative trigonal coupling derived here circumvents these difficulties, and is therefore a more likely possibility. The modified set of inter-planar coupling parameters for the trigonal coupling is given in Table I. The corresponding crystal-field parameters B_l^0 are derived from the low-temperature magnetization curves and T_C , and B_6^6 is determined so that the averaged bunching angle is 5.8° in the 12-layered structure in the low temperature limit. The values of these parameters are given in Table II, and they are close to those applied in the previous model.³⁸

The variation of the ordering vector with temperature in Ho has been analyzed by Pechan and Stassis,⁴ who found that it agrees reasonably well with the prediction of the theory of Elliott and Wedgwood.⁴³ $\mathcal{J}(\mathbf{q})$ is proportional to the susceptibility of the conduction electrons, which depends strongly on the nesting between different parts of the Fermi surface. The super-zone energy gaps created due to the oscillating polarization of the conduction electrons lead to a decrease of the maximum in the susceptibility and to a shift of its position towards smaller wave vectors, as the degree of polarization is increased. In addition, Andrianov⁴⁴ has discovered a relation, $\tau = \tau_0[(c/a)_{cr} - c/a]^{1/2}$, between the c/a -ratio and the ordering wave vector, where $(c/a)_{cr} \simeq 1.582$. This relation is obeyed nearly universally by the rare-earth metals, indicating a strong correlation between the c/a -ratio and the nesting

effects. A change of the c/a -ratio will modify the magnetic Hamiltonian in ways other than through $\mathcal{J}(\mathbf{q})$. B_2^0 is especially sensitive to the c/a -ratio, as to a first approximation it is proportional to the difference between c/a and its ideal value, and rather strong effects have recently been discovered in thulium, when the system jumps from the ferrimagnetic phase with $\tau = 2/7$ to the ferromagnetic structure.⁴⁵ In the model considered here we only account for the temperature variation in $\mathcal{J}(q)$, whereas additional magnetoelastic effects on the crystal-field parameters or changes of $\mathcal{J}(q)$ as a function of field are neglected. The spin-wave dispersion relation of Ho has been measured both at low temperatures^{38,46,47} and at elevated temperatures,⁴⁸ and these measurements have been used to derive the inter-planar exchange parameters.^{38,39} In order to reproduce the correct wave vectors at the different temperatures small adjustments have been introduced, and for this purpose we have chosen \mathcal{J}_3 as the variation parameter. The inter-planar exchange parameters used in the model are given in Table III.

The structures discussed in the next section have been calculated by a straightforward iteration procedure using the parameters given in Table I-III and Eqs. (2.3)-(2.4). The calculations utilize the mean-field approximation, in which $J_{\alpha i}J_{\alpha j}$ in (2.1) is replaced by $(2J_{\alpha i} - \langle J_{\alpha i} \rangle)\langle J_{\alpha j} \rangle$ and the trigonal term by Eq. (2.5). The first step in the iteration is to assume a distribution of expectation values of the various operators. These values are then inserted in the mean-field Hamiltonian for the i th ion, and after a diagonalization of this Hamiltonian the partition function, the free energy, and new expectation values for this ion are calculated. The calculation is carried out for each ion in one commensurable period, and the procedure is repeated with the new distribution of expectation values until a self-consistent solution is achieved. At a given temperature and field the free energies of structures with different (commensurable) periods are compared in order to identify the most stable structure. The energy differences between the various structures may be minute, and the calculations have to be done with high numerical accuracy. In order to ensure in a given case, that the iteration has converged towards the state with the lowest free energy and not to a metastable configuration, many iterations are required, of the order of several

thousands, and many starting configurations have to be considered.

III. THE COMMENSURABLE STRUCTURES

A. Low temperature regime

Most of the commensurable structures are observed in the low temperature regime ranging from zero to about 50 K. The exchange constants are given in Table III at the end points of this interval. In between we have used the quadratic interpolation:

$$J_n(T) = (1 - \alpha^2)J_n(0) + \alpha^2J_n(50 \text{ K}), \quad (3.1)$$

where α is the temperature T , in units of K, divided by 50.

At zero field the lowest order spin-slip structures are particularly stable. Starting at about 40 K, we get the sequence (221), (2221), (22221), (222221), corresponding to $\tau = 1/5, 4/21, 5/27$, and $2/11$, with a steady increase of the number of pairs in between the spin-slip layers as the temperature is reduced to about 20 K. One might expect this series to continue as the system is cooled further, but the $2/11$ -structure is predicted to occur only in a small temperature interval of about 0.8 K, and the intervals, where the subsequent spin-slip structures are stable, become minute. Thus the system is predicted to jump from the $2/11$ -structure to the pure pair-layered $1/6$ -structure within an interval of 0.1 K. Metastable states, or mixed states are expected to appear frequently in the real system, which makes it difficult to decide whether this particular prediction is in accord with the experiments, but the temperature interval, in which the indications^{11,13} of the intermediate structures are found is narrow with a width of about 1 K.

In addition to the lowest order spin-slip structures, structures with mixed sequences are also found to be stable. With one exception, the (222122221)-structure ($\tau = 3/16$), which is stable over a small interval of about 0.3 K, all the higher order spin-slip structures occur between the (221)- and the (2221)-structures, of which the most important one is the (2212221)-structure ($\tau = 7/36$). When approaching $\tau = 1/5$ from below, the main

sequence of commensurable ordering vectors is determined by $\tau_n(1) = n/(5n + 1)$ which is the series of rational fractions close to $1/5$ with the smallest denominators or shortest commensurable periods. Commensurable structures with wave vectors lying in between those determined by $\tau_n(1)$ may also be stable. In order to investigate this in a systematic way we have used the proposal of Selke and Duxbury that the structure most likely to appear between two phases has a period which is the sum of the periods of the structures in the two phases,^{33,49} suggesting that the most probable intermediate values in the present case are those determined by the second-order series $\tau_n(2) = (2n + 1)/(10n + 7)$. For a further subdivision of the steps made by τ we have applied the third-order series $\tau_n(3) = (3n + 1)/(15n + 8)$. In the interval between $\tau = 4/21$ and $\tau = 7/36$ the most stable configuration is found to be the $\tau_5(2) = 11/57$ or (22122212221)-structure, whereas other choices from the $\tau_n(1)$ or the $\tau_n(2)$ series are only found to be stable in narrow temperature intervals. For τ larger than $7/36$, the situation is changed. Structures defined by the series $\tau_n(1)$ as well as $\tau_n(2)$ are stable in about equal intervals, and for $n \geq 9$, structures determined by $\tau_n(3)$ also appear. At these temperatures the intervals are so small that it is difficult by the numerical calculations to distinguish the behavior from a truly continuous, incommensurable, variation of τ . The magnetic correlation length in the *c*-direction of Ho has been determined by x-ray scattering⁵⁰ to be of the order of 2000 layers, indicating that if the shortest commensurable period becomes of the order of 200 layers, it is no longer possible experimentally to distinguish commensurable ordering, repeating itself coherently about ten times, from an incommensurable phase. The non-zero resolution characterizing the numerical calculations is a limitation, when comparing the results with more exact analytic results, but not in a comparison with a real system, which suffers from impurities, stacking faults and other imperfections. Hence we expect that experimentally τ will change continuously, at least when it is larger than about 0.197 until it, at a first order transition, jumps to the commensurable value $\tau = 1/5$. The model calculations predict a lock-in at this wave vector between 41.47 K and 43.70 K, and that τ returns to incommensurable values above 43.70 K. The calculated results for the variation of τ at zero field, in the low

temperature regime, are shown in Fig. 1.

The stability of the different commensurable structures are influenced by a field along the c -axis. The calculations indicate that the main features of the phase diagram are the same as at zero field, but there are a few significant changes. There is an overall shift of the stable regimes of the commensurable structures towards lower temperatures, the more pronounced the lower the temperature is. The 2/11-phase and the spin-slip structures lying in between this phase and the 1/6-phase become more stable, until the field is so large that the overall temperature shift removes these phases, which happens between 25 and 35 kOe. Finally, the most important change is, that the stability of the $\tau = 1/5$ -phase is much increased by the field.

The first of these effects is explained by the condition that the moments in the spin-slip layers have a larger c -axis susceptibility than the moments in the pair layers, i.e. the more spin-slip layers a structure contains the more Zeeman energy it gains in a c -axis field. The experimental results of Cowley *et al.*,²⁷ obtained at a c -axis field of 10–50 kOe, which are included in Fig. 1, reflect this effect. Fig. 2 shows a more direct comparison of the experiments of Cowley *et al.* with the calculated field dependence of the ordering wave vector at 10 K. The experimental results shown in Fig. 2 are derived from the position of the primary magnetic satellite near (002), which leads to a more gradual change of the wave vector than if the contributions from different domains with different stable or metastable structures are separated, as shown in Fig. 1. The comparison in Fig. 2 demonstrates that the calculated shift of the ordering wave vector at a given temperature (i.e. at fixed values of the coupling constants) due to the c -axis field is of the same magnitude as observed experimentally. The calculated results at zero temperature are similar to the results in Fig. 2 at 10 K, except that the values of the transition fields are shifted upwards by about 5 kOe. The strong field-dependence of τ should be taken into consideration in the comparison between the experiments and the theoretical results in Fig. 1. In this comparison it may also be important that the 2/11-structure, in contrast to most of the other spin-slip structures, has a moment in the basal plane, and that the 3/16-structure, in between the 5/27- and the

4/21-structures, is much more susceptible to a basal-plane field than the two neighboring structures. This means that a small misalignment of the c -axis field would favor principally these two structures.

At not too high temperatures, the hexagonal anisotropy energy decreases with the relative magnetization, σ , proportional to approximately σ^{21} , whereas the trigonal anisotropy changes like σ^7 . The hexagonal anisotropy dominates at the lowest temperatures, and is responsible for the commensurable spin-slip structures, but as the temperature is increased the trigonal anisotropy becomes relatively more important. At 40 K $\sigma \simeq 0.925$, implying that the hexagonal anisotropy energy has decreased by a factor of 5 compared with its value in the zero temperature limit, whereas the trigonal anisotropy is only reduced by a factor of 1.7. Within perturbation theory the contribution of the trigonal interaction, Eq. (2.5), to the free energy is of second order in the helical phase, whereas a first-order contribution appears if the c -axis moments are nonzero. To a first approximation this contribution is proportional to

$$\Delta F \propto \sum_p (-1)^p J_{\parallel} J_{\perp}^3 \cos(3\phi_p), \quad (3.2)$$

where J_{\parallel} and J_{\perp} are the components of the moments parallel and perpendicular to the c -axis, respectively, and ϕ_p is the angle the perpendicular component of the moments in the p th layer makes with the x - or a -axis. When only the trigonal coupling is considered, then every second a -axis is an easy axis in one of the sublattices and the other three a -axes are the easy axes in the other sublattice. Fig. 3 shows the hodographs of the basal-plane moments calculated at 42.185 K in zero field and in the presence of a field of 10 kOe along the c -axis. The figure indicates that the three-fold anisotropy term induced by the c -axis field, (3.2), is capable of rotating the moments about 30°, so that the moments in the two spin-slip layers, which at zero field are along a b -axis become oriented along an a -axis. The hexagonal anisotropy energy does not depend on the distinction between the two sublattices and is changed by the same amount as obtained by rotating the zero-field hodograph the relatively small angle in the opposite direction. The small rotation does not cost much in

hexagonal anisotropy energy, whereas the gain in trigonal anisotropy energy is substantial.

Both structures in Fig. 3 look like spin-slip structures, except that the roles of the a - and the b -axes have been interchanged in the two cases. However, at these temperatures the basal-plane anisotropy energy is reduced so much that the spin-slip model is no longer particularly useful, since the angle between the moments in the pair layers is not much smaller than the smallest angle between moments belonging to neighboring pairs. The commensurable structures with τ slightly different from $1/5$ are not spin-slip structures. Instead they consist of portions of the $1/5$ -structure separated by domain walls in which phase shifts are introduced via a relatively smooth adjustment of the turn angles. If the width of the walls is much smaller than the distance between them, then the coupling between the walls is negligible and the free energy changes linearly with the density of walls, corresponding to a linear variation of the free energy with τ . A detailed discussion of the behavior of systems with domain walls is given by Fisher and Szpilka.⁵¹ Fig. 4 shows the free energy calculated in the two cases, for various commensurable values of τ in the proximity of $\tau = 1/5$. In the case of $H_c = 10$ kOe, the free energy varies linearly between 0.198 and 0.2 and between 0.2 to 0.202, whereas the variation is parabolic at zero field, except that the free energy at $\tau = 1/5$ is slightly smaller than the minimum value of the parabola. Leaving out the result at $\tau = 1/5$, the free energies of the zero-field commensurable structures are fitted by a third degree polynomial with a standard deviation of about 10^{-7} meV, which is the curve shown in the figure, (the numerical accuracy by which the free energy is calculated is 10^{-8} - 10^{-9} meV). This smooth change of the free energy is consistent with the estimated incommensurable variation of τ on both sides of the temperature interval where the $\tau = 1/5$ -structure is stable. The free energy in the zero field case is nevertheless going to change linearly with τ for τ sufficiently close to $1/5$, when $|\tau - 1/5|$ is smaller than about 0.0007.

The difference between the behavior of the free energy at zero and at $H_c = 10$ kOe is related to the different widths of the domain walls. Fig. 5 shows the turn angles in the two cases calculated at 42.815 K. In both cases τ is slightly smaller than $1/5$ corresponding to an average turn angle slightly smaller than 36° . The width of the domain walls, denoted by

the arrows, is about 100 layers in zero field and about 70 layers at $H_c = 10$ kOe. However, the phase shift accomplished by one domain wall is different in the two cases: 12° in the zero-field case and 24° , a factor 2 larger, in the case of $H_c = 10$ kOe. These numbers imply that the domain walls at zero field start to overlap with each other when $1/5 - \tau$ is larger than 0.0007, whereas when $H_c = 10$ kOe the overlap starts to occur only when $1/5 - \tau$ is nearly a factor of 3 larger. These same numbers also describe the situation at τ -values larger than $1/5$.

At decreasing temperatures the slope of the linear section in the free energy decreases, numerically, for τ smaller than $1/5$, and the opposite for τ larger than $1/5$. The $1/5$ -phase is the stable one until the temperature is lowered to the point where the slope becomes zero. At this temperature it costs no energy to create domain walls, as long as the distance between them is larger than their width. This leads to a vertical decrease of the τ -value at this temperature. At a slightly lower temperature the density of the domain walls will be so large that the walls overlap each other, and there will be only one equilibrium configuration, corresponding to the curvature in the free-energy function at the minimum being non-zero. The change of τ as a function of temperature will accordingly be more gradual. The transition between the $1/5$ -structure and other structures is predicted to occur in a (quasi)continuous⁵¹ way in both the cases considered, but at zero field the transition regime is so narrow that the transition is indistinguishable from a first-order one, within the present numerical resolution.

The lock-in of the structure at $\tau = 1/5$ is strongly enhanced by the c -axis field. As shown in Fig. 6, the interval in which the $1/5$ -structure is calculated to be stable increases rapidly, from about 2.2 K to about 10 K, between zero and a field of 10 kOe along the c -axis. This strong increase is also perceptible on either side of the $1/5$ -phase. Here commensurable effects are resolved even very close to the transition regions at 10 kOe, in contrast to the incommensurable behavior indicated by the calculations at zero-field. The large field-induced enhancement of the commensurable effects is produced solely by the trigonal coupling. We have repeated the calculations using the previous model³⁸ which neglects the trigonal cou-

pling. In this case the zero-field structure is found to be stable within an interval of 2.8 K, and this interval is reduced in a *c*-axis field, by a factor of 2 at a field of 30 kOe. The effective hexagonal anisotropy decreases faster than the free-energy differences between the different structures when the basal-plane moments are reduced by the field.

Tindall *et al.*²² have observed a plateau in the variation of τ at 1/5 over a temperature range of 2–3 K when $H_c = 30$ kOe, see Fig. 1, which disappears at zero field. It is probably very difficult to obtain experimental results on commensurable effects which can be trusted quantitatively in a comparison with the results derived from a mathematical model of an ideal system. The commensurable effects are based on very small differences in the free energy and impurities and defects are likely to be important. Furthermore, the results of Cowley *et al.*²⁷ in Fig. 1 show that, at low temperatures, several metastable configurations may be present in the crystal at the same time. The occurrence of metastable structures should be most pronounced at low temperatures, as also indicated by the behavior of the hysteresis effects, however, mixed phases are still observed at 35 K, see Fig. 1. Taking these effects into consideration, it seems reasonable that the calculated lock-in at zero-field of the 1/5-structure within an interval of about 2 K, may be smoothed out in the temperature variation of the average position of the fundamental magnetic scattering peak. We may instead refer to the low-field anomalies observed near 40 K in ultrasonic¹³ and magnetization¹⁵ measurements. The observed field enhancement of the lock-in of the 1/5-phase is in contradiction with the behavior expected if the trigonal coupling were negligible. Zeeman effects due to a small misalignment of the *c*-axis field are estimated to be of no importance, so, qualitatively, the enhancement may only be explained by the trigonal coupling. The question left open is whether the observed plateau of about 2 K at 30 kOe is consistent with the calculated range of the lock in of about 10 K.

B. High temperature regime

The high temperature regime is here considered to extend from 40–50 K and up to T_N . In this temperature range the anisotropy within the basal plane is relatively weak, and the spin-slip model no longer applies. Instead the additional anisotropy introduced by an external field will play a much more important role. The value of τ changes continuously in most of the interval, and detectable commensurable effects are only expected for structures with short commensurable periods, and we have limited ourselves to the study of the following three cases; the 18-layered 2/9-structure, the 8-layered 1/4-structure, and the 36-layered 5/18-structure appearing respectively around 75 K, 100 K, and 130 K.

Assuming the average slope $d\tau/dT$ near 75 K to be 0.001 K^{-1} , we calculate the lock-in interval of the 2/9-structure to be 0.5 K at zero field. This value is nearly unchanged in a field of 30 kOe along the c -axis. According to the magnetization measurements the transition to the fan structure, via intermediate helifan structures, occurs at a field of about 18 kOe applied along a b -axis.^{52,12} At 14 kOe the system is still in the helical phase, but the helix is strongly distorted by the field, the magnitude of the second (or seventh) harmonic of the basal-plane moments has grown to be almost the same as in the fan phase, and the 2/9-structure is found to be stable in an interval of 3.6 K. These commensurable effects for the 2/9-structure are found to be nearly independent of the trigonal anisotropy. The only weak tendency for the system to lock in at $\tau = 2/9$ at zero field or in the presence of a c -axis field seems to be in accordance with experiments. Tindall and collaborators have not reported any lock in of the 2/9 structures in these two cases, whereas they observed a plateau in the τ variation with a width of about 2 K in the presence of a b -axis field of 14 kOe,²⁴ which is consistent with the calculated behavior.

In the helical phase, the field perpendicular to the helical axis leads to a slight reduction of the τ -value. The transition to the fan-phase is accompanied by a further reduction of τ , hereafter in the fan phase there is a steady increase of τ with increasing field until the system becomes ferromagnetic. The possibility that the ordering wave vector may change

was not included in the original analysis of the helix-fan transition by Nagamiya *et al.*⁶ It has been observed by Koehler *et al.*⁵ at 50 K, where τ changes from 0.208 at zero field to be 0.170 in the fan phase, a change which was found to agree with the model calculations.⁷ At 80 K τ is about 0.230 at zero field and is calculated to be reduced to 0.199 when the helical structure is changed into a fan at 18 kOe. In the fan phase τ increases and is 0.222 at 30 kOe at the transition to the ferromagnet. The magnitude of these changes in τ decreases linearly with increasing temperatures and is a factor of 3 smaller at 100 K. This means that the temperature dependence of τ in the interval between 80 and 100 K is a factor of 2 larger at a field of 20 kOe, just above the helix-fan transition, than at zero field. This prediction may be compared with the experimental results of Tindall *et al.*²¹ shown in Fig. 5 of their paper. This figure shows that τ changes from about 0.18 at 81 K to about 0.23 at 95 K, when a field of 30 kOe is applied along a *b*-axis. This change is a factor of 3 larger than indicated by the calculation at 30 kOe, but it is comparable with the prediction at 20 kOe. In the fan phase the average basal-plane moment is about $6 \mu_B$, which leads to a demagnetization field in the case of a sphere of about 8 kOe, and it is therefore quite likely that the applied field of 30 kOe should be reduced by about 10 kOe in the comparison with the model calculations. Domain effects combined with the large value of the demagnetization field may also be the reason why Tindall *et al.*²¹ observed the magnetic satellite to split into two peaks in some of the scans, the observed splitting in τ of 0.007 corresponds to a field difference of 4–5 kOe. Tindall *et al.* do not report any particular lock-in effects for the structures shown in their Fig. 5. This is consistent with the model calculations which also do not indicate any significant commensurable effects for these structures.

The change of τ as a function of a basal-plane field is still of some magnitude around 100 K, and the calculated effect agrees well with the observation of Venter *et al.*²⁵ At 100 K the helix-fan transition is predicted to occur at a field of 18 kOe. At fields just below this value the 1/4-phase is found to be stable within an interval of about 2 K, the interval is 2.0 K at 16 kOe assuming $d\tau/dT = 0.00128 \text{ K}^{-1}$, whereas this interval is reduced by a factor of two or more in the fan phase. Tindall *et al.*^{19,21,24} have observed a lock-in of the 1/4-structure

in an interval of about 1 K at 14 kOe and about 1.5 K at 30 kOe, and Venter *et al.*²⁵ have made the similar observation that the 1/4-structure is stable within an interval of about 1 K at $H_b = 17$ and 23 kOe. The system is most likely to be still in the helical phase at 14 and 17 kOe. The positions of these lock-ins, just below 100 K in both cases, and their widths are in good agreement with that predicted in the helical case. The present model indicates that the stability of the 1/4-structure should decrease when the system jumps into the fan-phase, which is somewhat in disagreement with the experiments. We have two remarks to add to this minor discrepancy. Firstly, the (effective) anisotropy parameters are determined from the behavior of the system at low temperatures, and their values may have changed at these high temperatures. An increase of the axial anisotropy B_2^0 stabilizes the 1/4-structure in the fan phase, but does not have much effect on the helical structure. Secondly, it is uncertain whether the system is in the fan phase at the fields of 23 and 30 kOe. The relatively large demagnetization field in the case of the fan may lead to a mixing of the phases, and in addition there is the likely possibility that the structures are helifans,⁷ in which case the commensurable effects are larger than they would be in the fan phase.

Around 100 K the hexagonal anisotropy energy is very small and the calculations indicate that the basal-plane turn angle at zero field only differs by up to 0.12° from the average value of 45° for the 8-layered, $\tau = 1/4$, structure at zero field. The application of a field along the *c*-axis implies that the first-order trigonal contribution, Eq. (3.2), becomes non-zero and the trigonal anisotropy leads to a variation of the turn angle between 44.5° and 45.5° at $H_c = 30$ kOe. This modification is still small, and the model calculations indicate only very weak commensurable effects, a lock-in temperature interval of the order of 0.1 K both at zero field and when $H_c = 30$ kOe. In analogy with the fifth and seventh harmonics induced by the hexagonal anisotropy, the first-order trigonal anisotropy induces a second and a fourth harmonic, but because of the factor $(-1)^p$ in Eq. (3.2) these harmonics are translated by a reciprocal lattice vector along the *c*-axis (the half of a reciprocal lattice vector in the double-zone scheme), which means that the fourth harmonic appears at zero wave vector when $\tau = 1/4$. In other words, in the case of a cone structure with $\tau = 1/4$ the trigonal

coupling leads to a ferromagnetic component perpendicular to the cone axis. The two extra peaks observed in the cone phase in, for instance, the 2/11-structure³⁶ may be classified as arising from these harmonics, and in the cone phase of erbium, where $\tau = 5/21$ is close to $1/4$, the fourth harmonic is observed close to the nuclear peak,⁵³ see also the discussion in Ref. [42]. In the present case the ferromagnetic moment is along a b -axis and is calculated to be $0.043 \mu_B$ when $H_c = 30$ kOe, corresponding to an average rotation of the moments towards the b -axis by about 0.4° .

The estimated moment is small, but the energy differences determining the commensurable effects are also small, and the basal-plane moment has a profound influence on the system, as soon as the field has a non-zero component perpendicular to the c -axis. The Zeeman energy gained by the 1/4-structure, in comparison with the neighboring structures, is proportional to the angle θ between the c -axis and the direction of the field, at small values of the angle. At the temperature where the $\tau = 1/4$ structure is stable at $\theta = 0$, the free energy of the structures increases quadratically with $\tau - 1/4$, which leads to a lock-in temperature interval, ΔT , of the 1/4-structure proportional to $\sqrt{\theta}$. In this simple estimate we have neglected the small commensurable effect at $\theta = 0$, and the possibility that the structures with τ slightly different from $1/4$ may be able to develop a net moment in the basal plane. The size of the effect is illustrated in Fig. 7, which shows the calculated lock-in interval as a function of θ in a field of 30 kOe. ΔT increases like $\sqrt{\theta}$ at small values of θ and is about 12 K at $\theta = 30^\circ$. Between 30° and 40° the helix is only stable in part of the interval and is replaced by the fan structure in the other part. For θ larger than about 40° only the fan is stable and ΔT decreases to about 1 K at 90° . As mentioned above the hexagonal anisotropy is very small at these temperatures and for θ larger than about 0.5° the results shown in Fig. 7 are independent of whether the field is lying in the $a-c$ or the $b-c$ plane. The transitions between the 1/4-structure and the surrounding incommensurable structures are established via the creation of domain walls and are continuous, equivalently to the case of τ close to $1/5$.

The vertical slope of ΔT as a function of θ at the origin means that even the slightest

deviation of the field from perfect alignment along the c -axis will produce a sizable lock-in effect, e.g. ΔT is calculated to be 2.7 K at $\theta = 1^\circ$ when $H = 30$ kOe. Both this value and the very weak lock-in effect at zero field are in good agreement with the observations made by Noakes, Tindall and collaborators,^{16,17} who saw no sign of a lock-in at zero field but detected plateaus at $\tau = 1/4$ with a temperature range of 2–2.5 K in a c -axis field of 17–30 kOe. The lock-in effect is independent of the direction of the field component in the basal plane, but it is not necessarily easy for the 1/4-structure to adjust itself to even a slow spatial variation in the direction of the field, because a rotation of the ferromagnetic moment in the basal plane requires a shift in the (average) phase angle for the 1/4-structure which is about one quarter of the angle the moment is rotated. This effect, in combination with the presence of magnetic domains, may explain why Venter *et al.*²⁵ did not detect any clear plateau at $\tau = 1/4$ in a c -axis field.

The mean-field properties of the 36-layered, $\tau = 5/18$, structure just below the Néel temperature have also been investigated. At zero field and at a temperature of 125 K, the model predicts only a marginal lock-in effect, of the order of 0.05 K. The calculations indicate an increase of the effect when a field is applied in the basal plane, but the increase is not substantial, only about a factor 1.5 in a field of 30 kOe. At this field it is assumed that the structure is a fan, as the helix-fan transition is estimated to occur at a field of about 20 kOe. The lock-in effects predicted at these temperatures are far below what might be considered to be observable effects, in contradiction with the experimental results. Neutron diffraction experiments show a clear lock-in effect for the 5/18-structure between 126 K and $T_N \simeq 132.9$ K at a field of 30 kOe along the b -direction,^{21,23} which is accompanied by ultrasonic anomalies in the propagation of longitudinal sound waves along the c -direction.²⁶ This lock-in phenomenon so close to the ordering temperature lies outside the range of what might be explained by a mean-field model. In the mean-field approximation the anisotropy energies are nearly eliminated close to T_N due to thermal fluctuations. However, it might be possible that these fluctuations behave somewhat systematically such as to favor commensurable structures, analogously to the commensurable effects induced by quantum fluctuations

according to the analysis of Harris *et al.*⁵⁴

IV. DISCUSSION AND CONCLUSION

The most important result of the present investigation of the commensurable structures in holmium is that the increased stability of the 10-layered periodic structure around 42 K and of the 8-layered periodic structure around 96 K, observed when applying a field along the *c*-axis, can be understood. In both cases the explanation relies totally on the trigonal coupling, adding to the evidence for the presence of this coupling in holmium. The two cases are also the only ones found where the trigonal coupling has any significant effect on the stability of the commensurable structures.

With a few exceptions the calculated ranges in which the different commensurable structures are stable, are larger than indicated by the experiments, and these differences are most noticeable at low temperatures. This may be explained by the occurrence of metastable structures in the samples. The neutron diffraction experiments of Cowley *et al.*²⁷ show that the crystals may contain several domains with different structures below 40 K. As the temperature is raised the energy barriers between the metastable structures decrease and the thermal energies increase, so that the system may more easily reach thermal equilibrium. At low temperatures, in the regime of the spin-slip structures, there is the additional possibility that the regularly spaced spin-slip layers in the equilibrium state are disordered to some extent. The x-ray diffraction measurements of Helgesen *et al.*⁵⁰ indicate that this is the case. They have observed a reduction of the longitudinal correlation length between 40 and 20 K by a factor of three, a reduction which is partly removed when the spin-slip layers disappear at the lock-in transition to $\tau = 1/6$ at about 20 K.

The only indisputable discrepancy between the theory and the experiments is found in the behavior displayed by the 5/18-structure. The experiments^{21,23,26} indicate that this structure locks-in between 126 K and T_N in a *b*-axis field of 30 kOe, whereas the calculations only show a marginal effect. This discrepancy does not necessary question the model, but

is more likely a consequence of the limited validity of the mean-field approximation close to the magnetic phase transition. The fluctuations neglected in the calculations may be so large in this case that their contribution to the free energy is decisive for the commensurable effects.

At temperatures well below T_N we do not expect any major corrections to the lock-in intervals derived in the mean-field approximation. Any discrepancy would rather be due to a failure of the model than to the use of this approximation. The model does not include magnetoelastic effects, except implicitly through the variation of $\mathcal{J}(q)$. The temperature dependence of the exchange interaction, which is accounted for in a phenomenological way in consistency with the behavior of the spin-wave energies, may relate to changes of the c/a -ratio.⁴⁴ The magnetoelastic effects in holmium, like in the other rare-earth metals, are important, but they do not seem to have much direct influence on the lock-in phenomena. Possible exceptions are the cases of the $\tau = 2/11$ and $3/16$ spin-slip structures, which both have the distinct property that the averaged value of the quadrupole moments in the basal plane is non-zero. The neglect of magnetoelastic effects in the model implies that all the parameters are assumed to stay constant as functions of the field, at a fixed temperature. A field dependence of $\mathcal{J}(q)$ is expected based on the Elliott–Wedgwood theory,⁴³ because the polarization of the conduction electrons is changed by the field. It is therefore interesting to notice that the model is able to account for most of the field dependence of the ordering wave vector in holmium, observed both at low temperatures and at temperatures around 80–100 K, without much need for invoking a field-dependence of the exchange coupling.

The trigonal coupling derived in the present analysis, is somewhat smaller than the coupling considered by Simpson *et al.*,³⁶ and in comparison with the exchange coupling its relative magnitude is ten times smaller in holmium than in erbium.⁴² Nevertheless, the two commensurable effects in holmium determined by the trigonal coupling are found to be very pronounced, and a more detailed experimental investigations of these two effects would be valuable. The lock-in temperature interval of the 1/5-structure is predicted to be larger than indicated by the variation in the position of the first harmonic,^{16,17} and a study of the

behavior of the fifth or seventh harmonics will be useful for a clarification of the experimental situation. The strong lock-in of the 1/4-structure around 96 K indicated by the mean-field model, Fig. 7, deserves further studies, in which the field is applied by purpose in a direction making a non-zero angle with the *c*-axis, or with the basal-plane.

ACKNOWLEDGMENTS

The author wants to express his gratitude to Allan R. Mackintosh who tragically died after a car accident. He was always extremely helpful and full of insight, and the author and many others have benefited from discussions with him on problems in physics. We will all remember and miss his enthusiasm and deep understanding of the physics of metals and of the rare earths.

REFERENCES

¹ W. C. Koehler, J. W. Cable, M. K. Wilkinson and E. O. Wollan, Phys. Rev. **151**, 414 (1966).

² K. Yosida, in *Progress in low temperature physics IV* (Ed. C. J. Gorter) (North-Holland, Amsterdam), 265 (1964).

³ G. P. Felcher, G. H. Lander, T. Ari, S. K. Sinha and F. H. Spedding, Phys. Rev. B **13**, 3034 (1976).

⁴ M. J. Pechan and C. Stassis, J. Appl. Phys. **55**, 1900 (1984).

⁵ W. C. Koehler, J. W. Cable, H. R. Child, M. K. Wilkinson and E. O. Wollan, Phys. Rev. **158**, 450 (1967).

⁶ T. Nagamiya, K. Nagata and Y. Kitano, Prog. Theor. Phys. **27**, 1253 (1962).

⁷ J. Jensen and A. R. Mackintosh, Phys. Rev. Lett. **64**, 2699 (1990).

⁸ D. A. Jehan, D. F. McMorrow, R. A. Cowley and G. J. McIntyre, Europhys. Lett. **17**, 553 (1992); D. A. Jehan, D. F. McMorrow, R. A. Cowley and G. J. McIntyre, J. Magn. Magn. Mat. **104-107**, 1523 (1992).

⁹ D. Gibbs, D. E. Moncton, K. L. D'Amico, J. Bohr and B. H. Grier, Phys. Rev. Lett. **55**, 234 (1985).

¹⁰ J. Bohr, D. Gibbs, D. E. Moncton and K. L. D'Amico, Physica A **140**, 349 (1986).

¹¹ R. A. Cowley and S. Bates, J. Phys. C **21**, 4113 (1988).

¹² A. R. Mackintosh and J. Jensen, in *Disorder in Condensed Matter Physics* (Eds. J.A. Blackman and J. Taguena) (Oxford University Press, Oxford), 213-30 (1991).

¹³ S. Bates, C. Patterson, G. J. McIntyre, S. B. Palmer, A. Mayer, R. A. Cowley and R. Melville, J. Phys. C **21**, 4125 (1988).

¹⁴ M. O. Steinitz, M. Kahrizi, D. A. Tindall and N. Ali, Phys. Rev. B **40**, 763 (1989).

¹⁵ F. Willis, N. Ali, M. O. Steinitz, M. Kahrizi and D. A. Tindall, J. Appl. Phys. **67**, 5277 (1990).

¹⁶ D. R. Noakes, D. A. Tindall, M. O. Steinitz and N. Ali, J. Appl. Phys. **67**, 5274 (1990).

¹⁷ D. A. Tindall, M. O. Steinitz, M. Kahrizi, D. R. Noakes and N. Ali, J. Appl. Phys. **69**, 5691 (1991).

¹⁸ M. O. Steinitz, D. A. Tindall and M. Kahrizi, J. Magn. Magn. Mat. **104-107**, 1531 (1992).

¹⁹ D. A. Tindall, M. O. Steinitz and T. M. Holden, J. Phys. Condens. Matter **4**, 9927 (1992).

²⁰ D. A. Tindall, M. O. Steinitz and D. R. Noakes, Physica B **180&181**, 79 (1992).

²¹ D. A. Tindall, M. O. Steinitz and T. M. Holden, J. Appl. Phys. **73**, 6543 (1993).

²² D. A. Tindall, M. O. Steinitz and T. M. Holden, Phys. Rev. B **47**, 5463 (1993).

²³ D. A. Tindall, C. P. Adams, M. O. Steinitz and T. M. Holden, J. Appl. Phys. **75**, 6318 (1994).

²⁴ D. A. Tindall, C. P. Adams, M. O. Steinitz and T. M. Holden, J. Appl. Phys. **76**, 6229 (1994).

²⁵ A. M. Venter, P. de V. du Plessis and E. Fawcett, Physica B **180&181**, 290 (1992).

²⁶ A. M. Venter and P. de V. du Plessis, J. Magn. Magn. Mat. **140-144**, 757 (1995).

²⁷ R. A. Cowley, D. A. Jehan, D. F. McMorrow and G. J. McIntyre, Phys. Rev. Lett. **66**, 1521 (1991).

²⁸ M. E. Fisher and W. Selke, Phys. Rev. Lett. **44**, 1502 (1980).

²⁹ P. Bak and J. von Boehm, Phys. Rev. B **21**, 5297 (1980).

³⁰ P. Bak, Rep. Prog. Phys. **45**, 587 (1982).

³¹ J. Smith and J. M. Yeomans, *J. Phys. C* **16**, 5305 (1983).

³² K. Sasaki, *J. Stat. Phys.* **68**, 1013 (1992).

³³ F. Seno, J. M. Yeomans, R. Harbord and D. Y. K. Ko, *Phys. Rev.* **49**, 6412 (1994).

³⁴ M. O. Steinitz, D. A. Tindall and C. P. Adams, *J. Magn. Magn. Mat.* **140-144**, 759 (1995).

³⁵ M. L. Plumer, *Phys. Rev. B* **44**, 12376 (1991).

³⁶ J. A. Simpson, D. F. McMorrow, R. A. Cowley and D. A. Jehan, *Phys. Rev. B* **51**, 16073 (1995); J. A. Simpson, D. F. McMorrow, R. A. Cowley and D. A. Jehan, *J. Magn. Magn. Mat.* **140-144**, 751 (1995).

³⁷ J. Jensen and A. R. Mackintosh, *Rare Earth Magnetism: Structures and Excitations* (Oxford University Press, Oxford, 1991).

³⁸ C. C. Larsen, J. Jensen and A. R. Mackintosh, *Phys. Rev. Lett.* **59**, 712 (1987).

³⁹ J. Jensen, *J. Phys. (Paris)* **49** C-8, 351 (1988).

⁴⁰ J. Jensen and A. R. Mackintosh, *J. Magn. Magn. Mater.* **104-107**, 1481 (1991).

⁴¹ A. R. Mackintosh and J. Jensen, *Physica B* **180&181**, 1 (1992).

⁴² R. A. Cowley and J. Jensen, *J. Phys. Condens. Matter* **4**, 9673 (1992); J. Jensen and R. A. Cowley, *Europhys. Lett.* **21**, 705 (1993).

⁴³ R. J. Elliott and F. A. Wedgwood, *Proc. Phys. Soc.* **84**, 63 (1964).

⁴⁴ A. V. Andrianov, *Pis'ma Z. Exp. Teor. Fiz.* **55**, 639 (1992) [JETP Lett. **55**, 666 (1992)]; A. V. Andrianov, *J. Magn. Magn. Mat.* **140-144**, 749 (1995).

⁴⁵ K. A. McEwen, U. Steigenberger, L. Weiss, T. Zeiske and J. Jensen, *J. Magn. Magn. Mat.* **140-144**, 767 (1995).

⁴⁶ M. W. Stringfellow, T. M. Holden, B. M. Powell and A. D. B. Woods, *J. Phys. C* **2**, S189 (1970).

⁴⁷ C. Patterson, D. F. McMorrow, H. Godfrin, K. N. Clausen and B. Lebech, *J. Phys. Condens. Matter* **2**, 3421 (1990); D. F. McMorrow, C. Patterson, H. Godfrin and D. A. Jehan, *Europhys. Lett.* **15**, 541 (1991).

⁴⁸ R. M. Nicklow, *J. Appl. Phys.* **42**, 1672 (1971).

⁴⁹ W. Selke and P. Duxbury, *Z. Phys. B* **57**, 49 (1984).

⁵⁰ G. Helgesen, J. P. Hill, T. R. Thurston, D. Gibbs, J. Kwo and M. Hong, *Phys. Rev. B* **50**, 2990 (1994); G. Helgesen, J. P. Hill, T. R. Thurston and D. Gibbs, *Phys. Rev. B* **52**, 9446 (1995).

⁵¹ M. E. Fisher and A. M. Szpilka, *Phys. Rev. B* **36**, 644 (1987).

⁵² J. L. Féron, Thesis, University of Grenoble, 1969 (unpublished).

⁵³ H. Lin, M. F. Collins, T. M. Holden and W. Wei, *Phys. Rev. B* **45**, 12873 (1992).

⁵⁴ A. B. Harris, C. Micheletti and J. M. Yeomans, *Phys. Rev. Lett.* **74**, 3045 (1995).

TABLES

TABLE I. The trigonal coupling parameters (10^{-4} meV).

n	1	2	3
$[K_{31}^{21}]_n$	0.7	0.4	0.2

TABLE II. The crystal-field parameters (meV).

B_2^0	B_4^0	B_6^0	B_6^6
0.024	0.0	$-0.95 \cdot 10^{-6}$	$9.4 \cdot 10^{-6}$

TABLE III. The inter-planar exchange parameters (meV) as functions of temperature.

T [K]	\mathcal{J}_0	\mathcal{J}_1	\mathcal{J}_2	\mathcal{J}_3	\mathcal{J}_4	\mathcal{J}_5	\mathcal{J}_6
0	0.300	0.09	0.006	-0.0140	-0.006	-0.002	0.0
50	0.290	0.10	0.010	-0.0290	-0.005	0.008	-0.004
72	0.267	0.11	0.010	-0.0377	-0.001	0.004	-0.003
96	0.245	0.11	0.010	-0.0463	0.006	0.0	0.0
125	0.210	0.11	0.010	-0.0640	0.006	0.0	0.0

FIGURES

FIG. 1. The ordering wave vector in Ho as a function of temperature below 50 K. The calculated results are shown by the horizontal solid lines, which are connected with vertical thin solid or thin dashed lines corresponding respectively to the results obtained at zero or at a field of 10 kOe applied along the c -axis. The symbols show the experimental results of Cowley *et al.*²⁷ at various values of the c -axis field as defined in the figure. The thick dashed line, between 35 and 48 K, indicates the variation of τ derived by Tindall *et al.*²² from the position of the primary magnetic diffraction peak in a c -axis magnetic field of 30 kOe. The smooth curve shown by the thin solid line is the temperature dependent position of the maximum in $\mathcal{J}(q)$, as determined by Eq. (3.1).

FIG. 2. The ordering wave vector in Ho as a function of a c -axis field at 10 K. The solid line is the theoretical result, and the triangles pointing up or down are the experimental results of Cowley *et al.*²⁷ obtained at increasing or decreasing field values, respectively. The systematic difference between the two sets of results indicates that hysteresis effects are important. The experimental results are derived from the position of the principal magnetic satellite, and thus include implicitly an averaging of the ordering wave vector over the different domains.

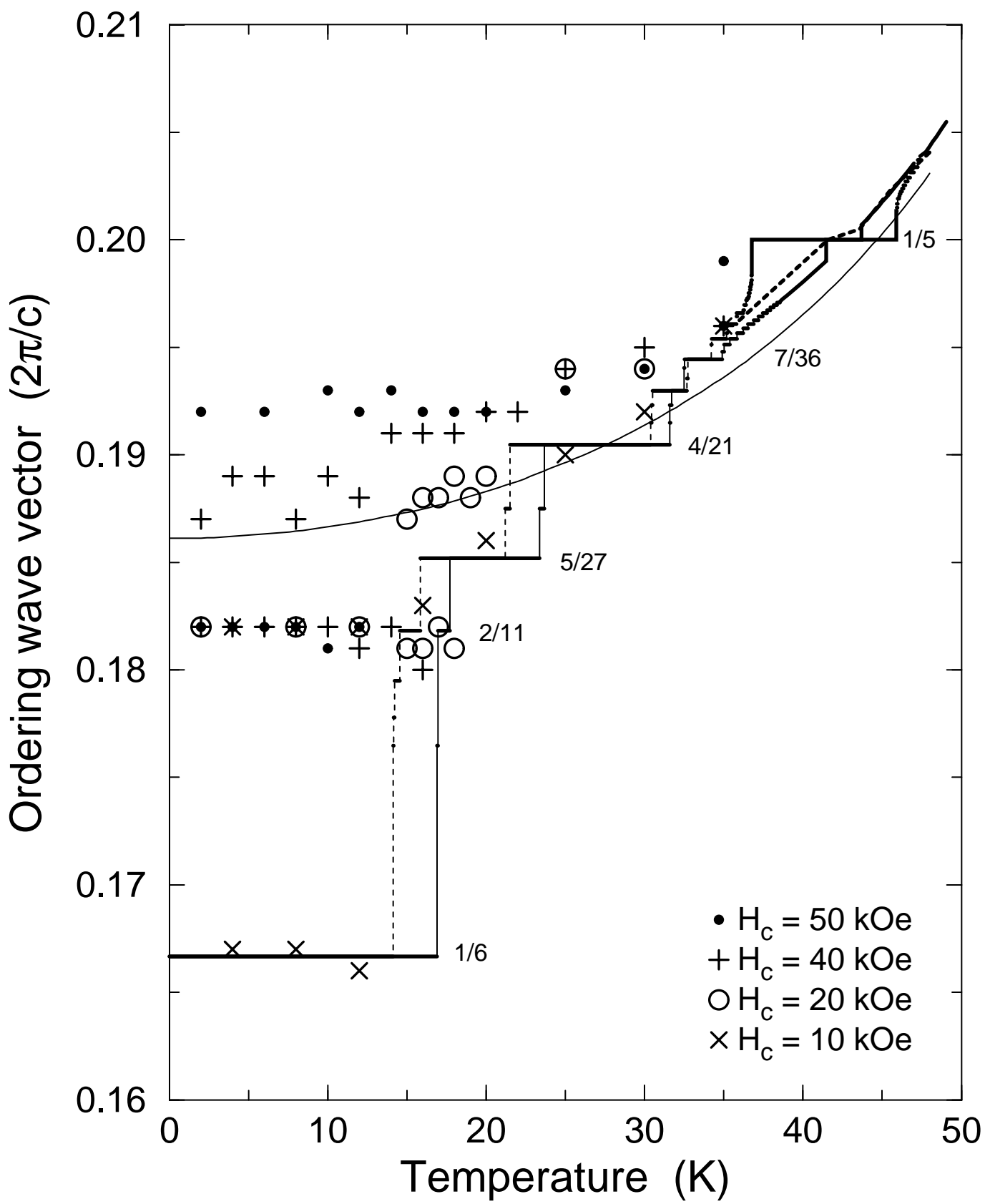
FIG. 3. The hodograph of the basal-plane moments of the 10-layered (221)-structure calculated at 42.185 K in zero field and in the presence of a field of 10 kOe along the c -axis. The two hodographs are rotated about 30° relatively to each other as indicated by the arrow.

FIG. 4. The free energy of the commensurable structures at 42.185 K as a function of the ordering wave vector calculated at zero field and at a field of 10 kOe applied along the c -axis. The energy scales used in the two cases are displaced with respect to each other as indicated on the figure. The plus signs denote the free energy of the structures calculated with commensurable periods between about 100 and 500 hexagonal layers.

FIG. 5. The turn angles of the moments in different hexagonal layers numbered along the c -axis, calculated at zero field and in the present of a c -axis field of 10 kOe at the same temperature, 42.185 K, as considered in the Figs. 3 and 4. The domain walls indicated by the arrows lead to negative phase shifts of the regular 1/5-structural parts on each side of the walls, which are 12° at zero field and 24° in the case of $H_c = 10$ kOe.

FIG. 6. The calculated lock-in temperature interval, ΔT , of the 1/5-phase as a function of the c -axis field.

FIG. 7. The calculated lock-in temperature interval, ΔT , of the 1/4-phase as a function of a field of 30 kOe applied in a direction making the angle θ with the c -direction. The midpoint of the interval is between 95–97 K in the helical case and lies between 102–100 K in the fan phase.



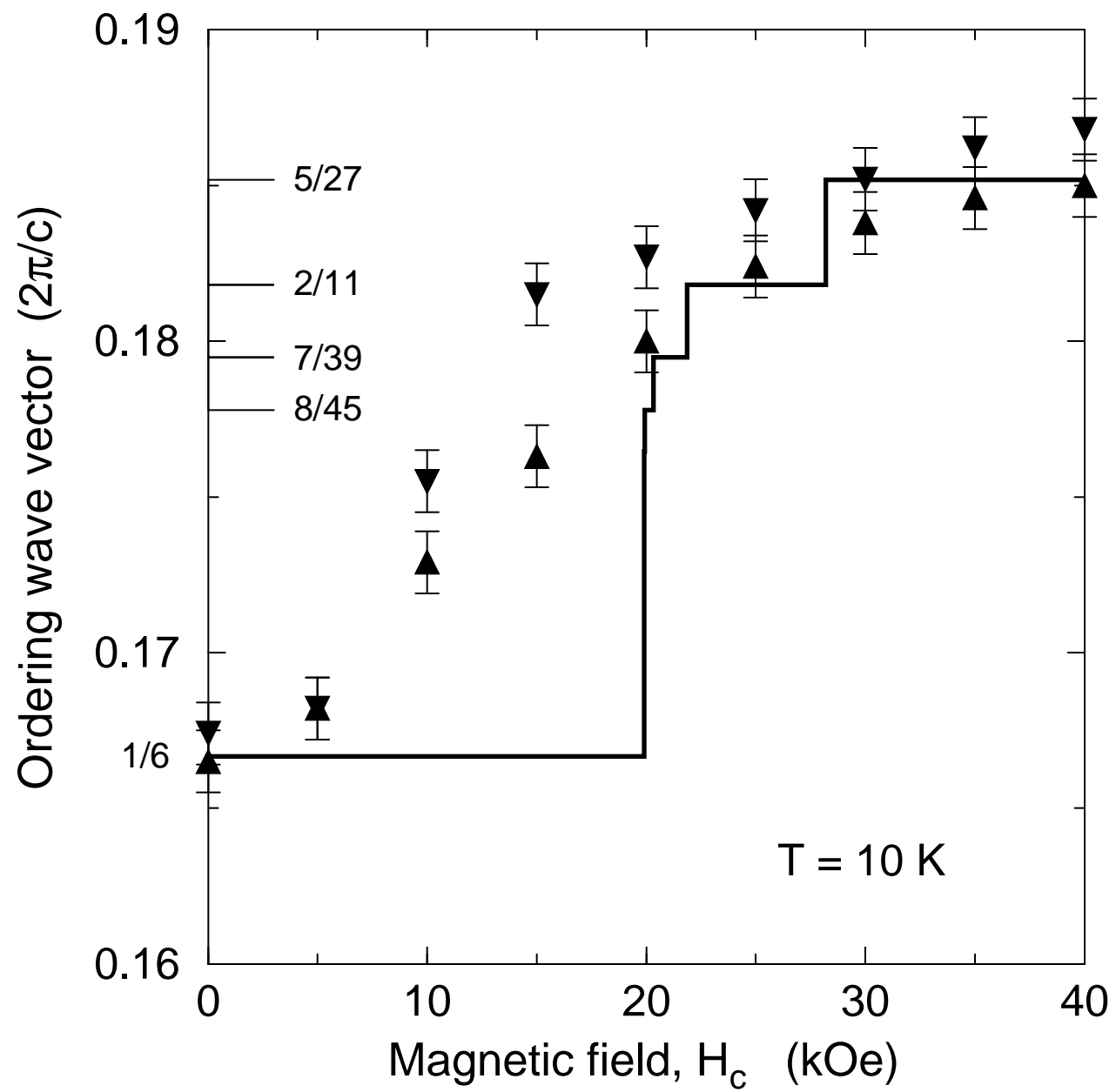


Fig. 2

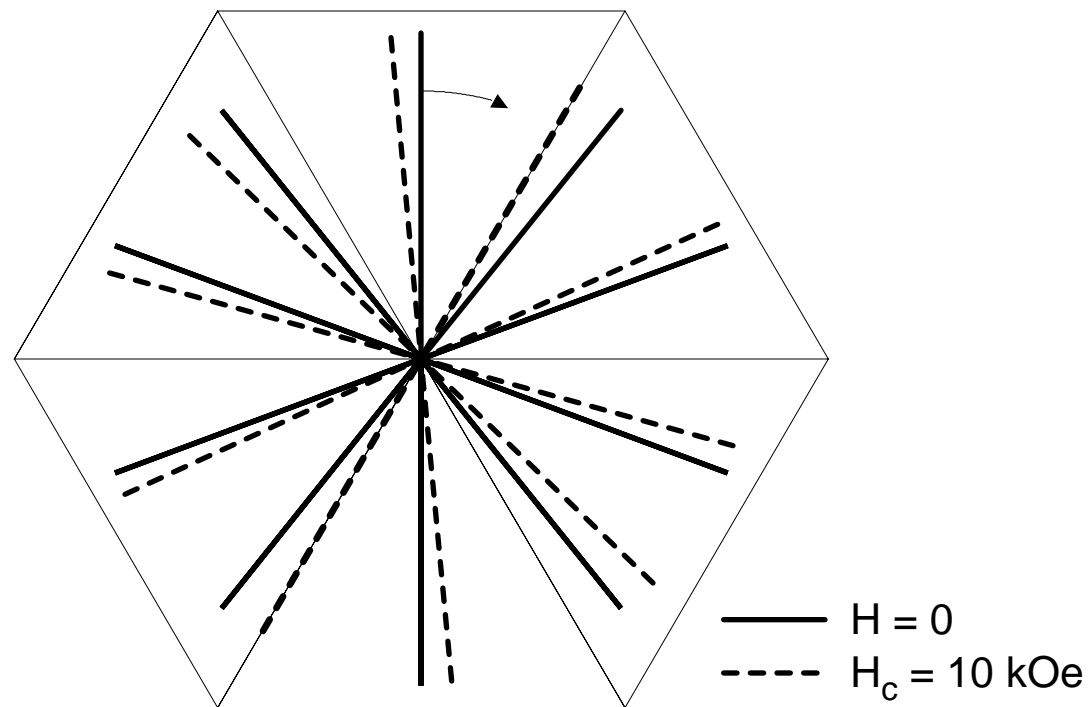


Fig. 3

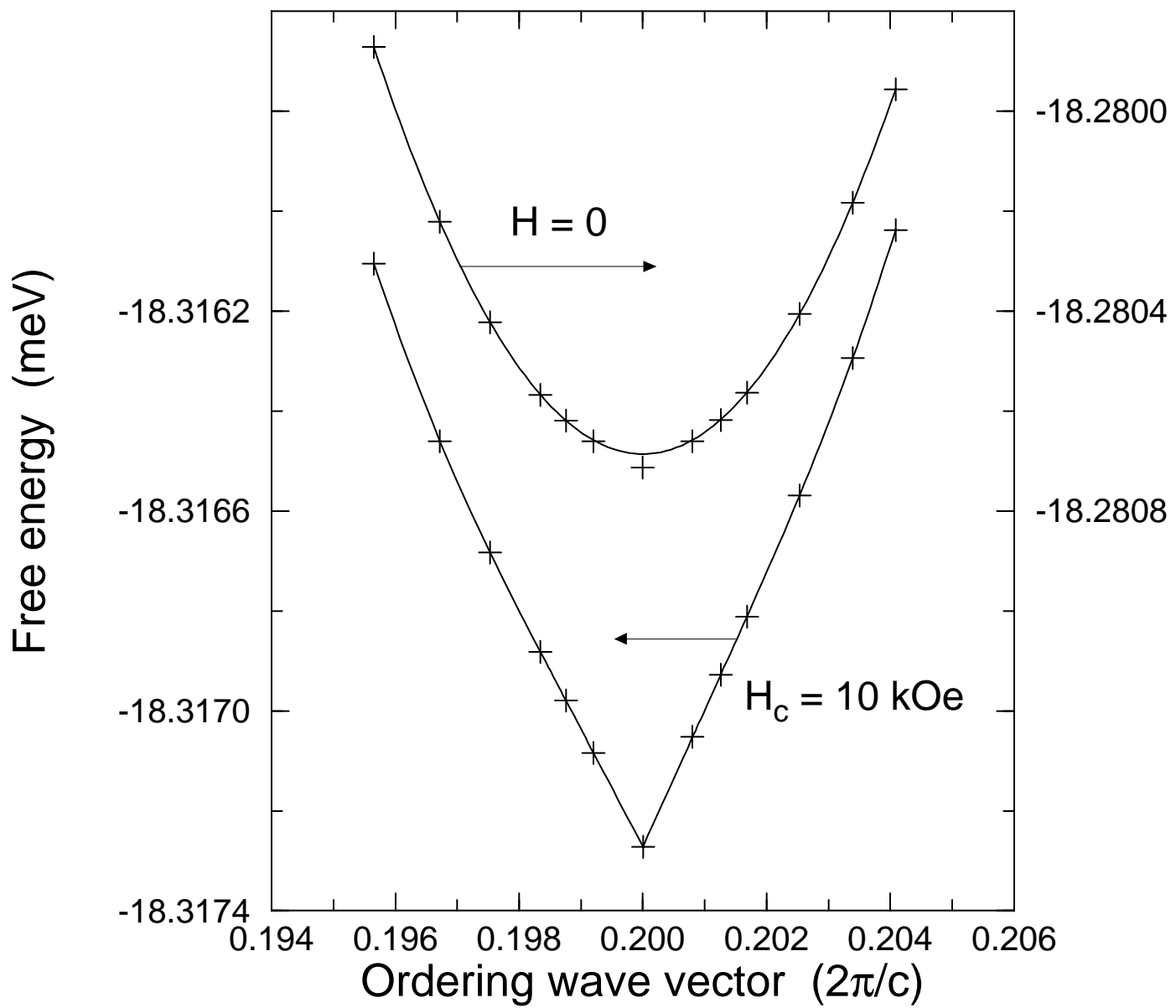


Fig. 4

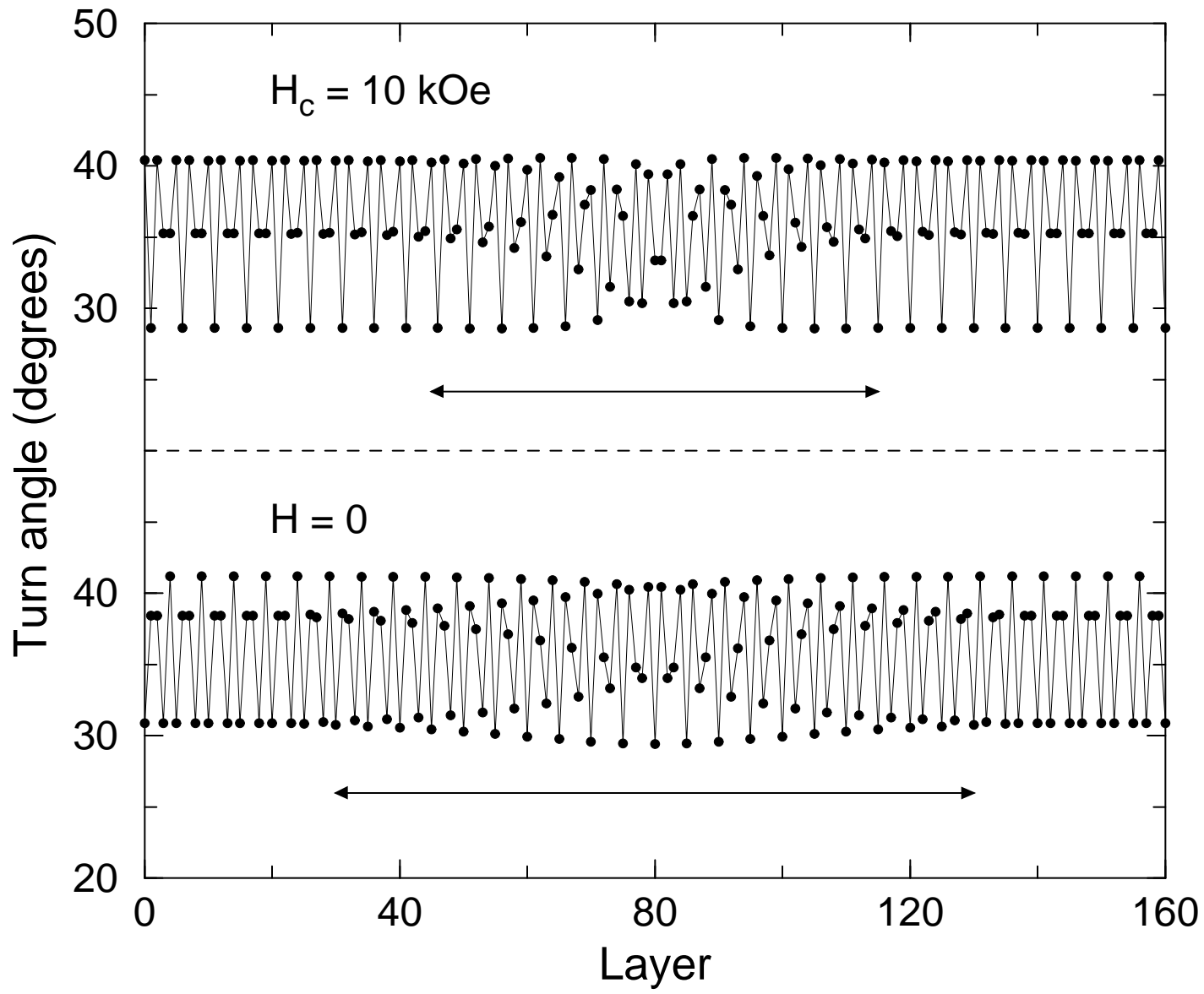


Fig. 5

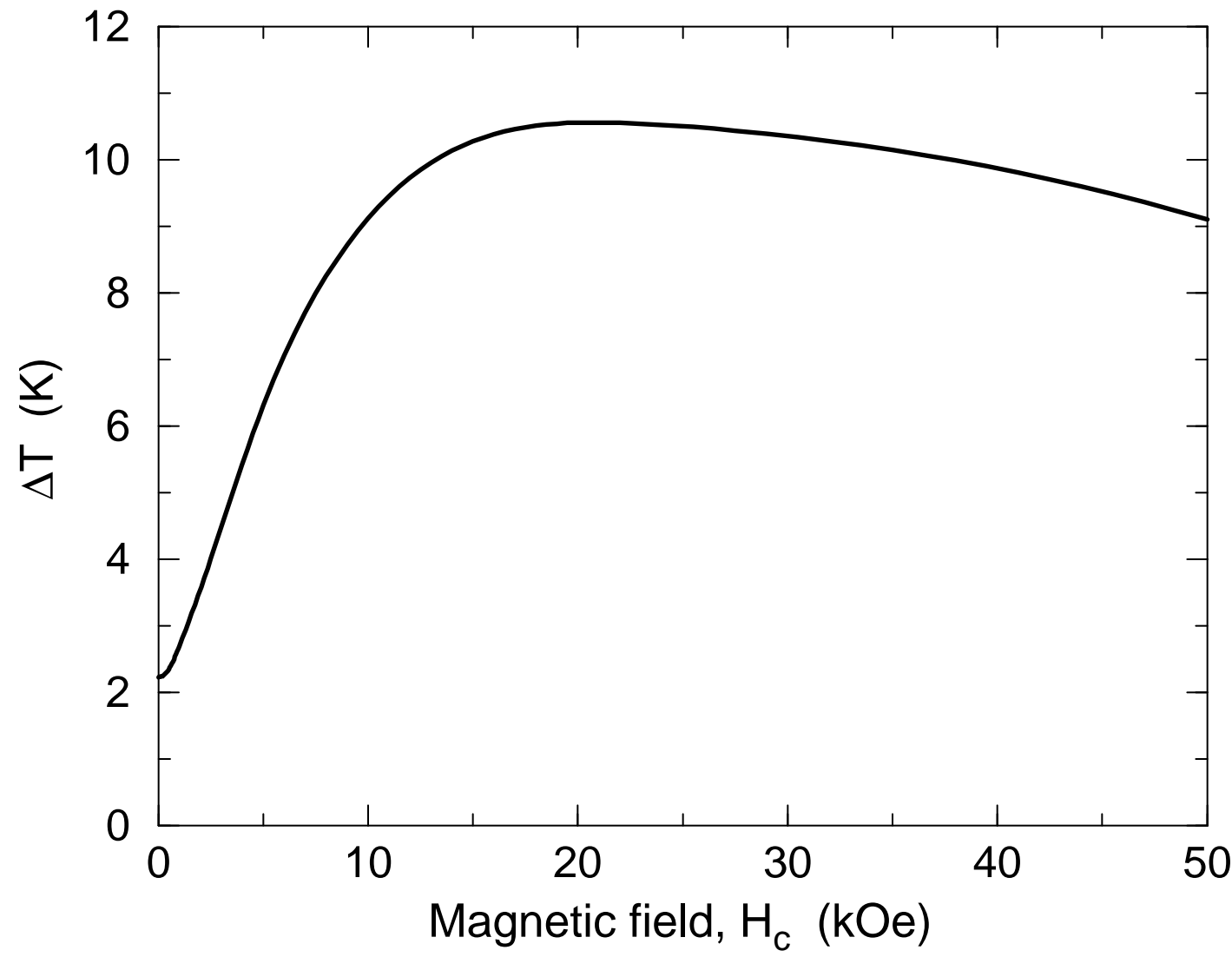


Fig. 6

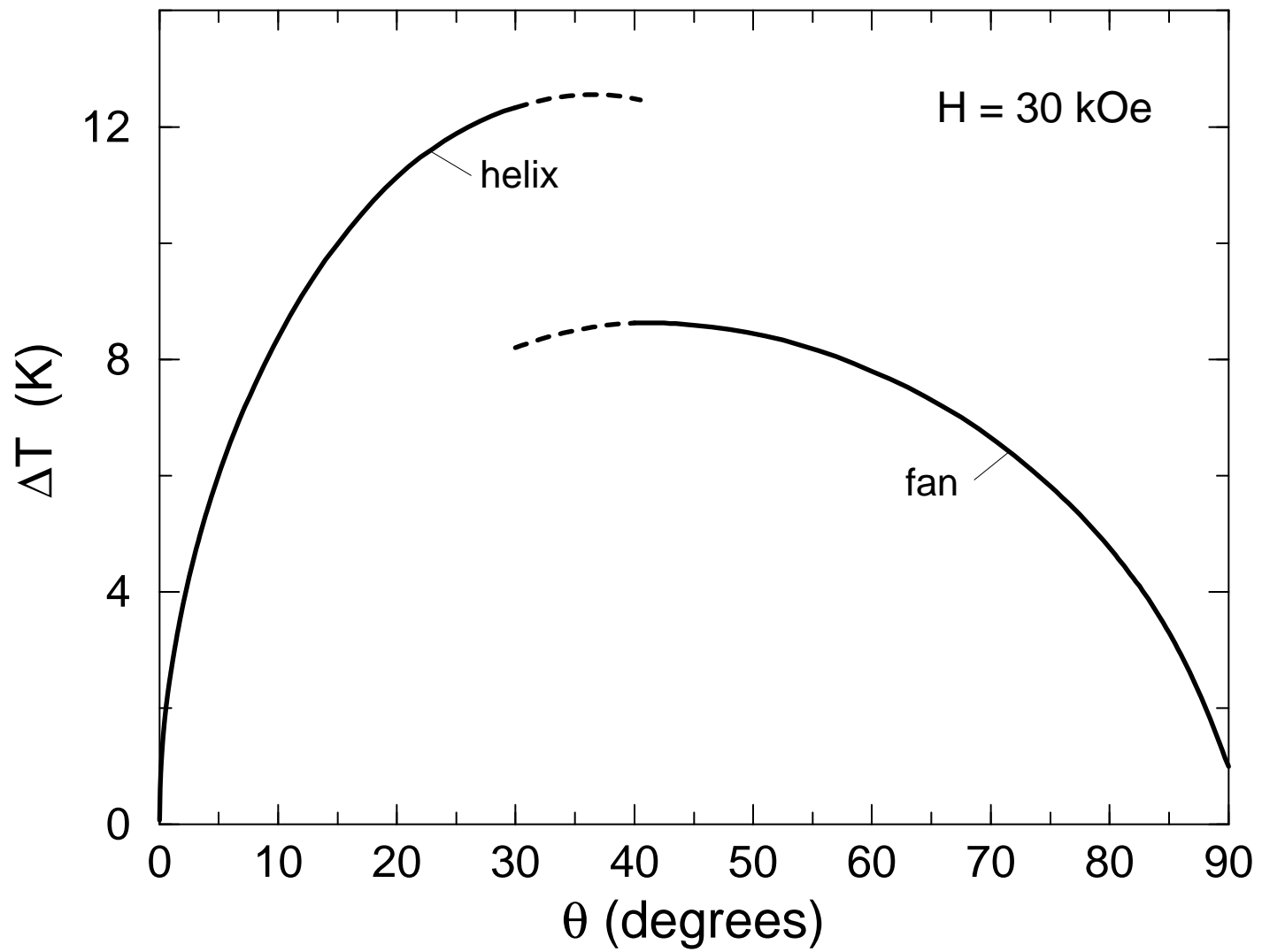


Fig. 7